# Reduced-Order Square-Root EKF for Sensorless Control of PMSM Drives

Václav Šmídl
Institute of Information Theory and Automation
Prague, Czech Republic
email: smidl@utia.cas.cz

Zdeněk Peroutka
Regional Innovation Centre for Electrical Engineering
University of West Bohemia
Pilsen, Czech Republic
email: peroutka@ieee.org

***Abstract*—Performance of square-root extended Kalman filter (EKF) based on reduced order models for sensorless control of permanent magnet synchronous motor (PMSM) drives is studied. The reduced order model of PMSM has two-dimensional state vector comprising of: (i) electrical rotor speed, and (ii) electrical rotor position. These state quantities are estimated by the EKF without either speed or position sensor on the motor shaft. The reduction of the model order results in dramatic speed-up of calculation of the estimator which takes only a few tens of microseconds on a conventional fixed-point digital signal processor. Accuracy of the estimator is improved using square-root representation of the covariance matrix. Due to its low computational requirements, the proposed square-root EKF estimator is eligible for sophisticated diagnostics as well for sensorless control of PMSM drive in a wide range of industrial applications. Presented theoretical conclusions are verified by both simulations and experiments carried out on developed PMSM drive prototype of rated power of 10.7kW.**

## I. Introduction

Sensorless control of an ac drive—i.e. it operation without either rotor position and/or speed sensor—can be achieved by many techniques, ranging from MRAS [1] to complex schemes. The Extended Kalman Filter (EKF) is a basis for many variants of sensorless control schemes using different models, e.g. [2], [3]. The common perception of EKF is that it is computationally expensive and thus unsuitable for a low-cost digital signal processor (DSP). A possible solution is to implement the EKF-based sensorless control on powerful floating-point DSPs or FPGAs [4]. Implementation of the EKF in a low-cost DSP with limited computational performance—which are at present used in ac electric drives from simple consumer electronics up to either traction or generally high-power drives—is much more demanding for two reasons. First, low-cost DSPs usually support only fixed-point arithmetics which implies limited dynamic range and scales, and therefore, reduced calculation accuracy. Second, reduction of computational cost motivates to replace full model of the drive by an approximation e.g. in the form of reduced-order model.

A principled solution to the first problem is based on square root decomposition of the covariance matrix [5], which has been applied to the sensorless control problem in [6]. The number of reduced order models offering potential solution to the second problem is rather wide. One possibility is to apply sophisticated techniques of projection of the full state-space model into lower dimensional state [7], [8], [9]. An alternative way is to interpret the standard state-space model in terms of back-emf equations, e.g. [10]. In this paper, we discuss the latter approach since it does not require any transformations or auxiliary variables. We focus our attention to implementation of the EKF in fixed-point arithmetics and discuss differences from the full state-space model. Specifically, we develop and compare the Bierman-Thorton variant of the square-root EKF [5].

This paper is organized as follows. The reduced order model is introduced in Section II. Details of fixed-point implementation of the square-root EKF are discussed in Section III. Details of the drive control strategy are presented in Section IV. The presented algorithms are in detail compared in simulations in Section V and on a laboratory prototype of sensorless PMSM drive of rated power of 10.7kW in Section VI.

## II. Reduced Order Model of PMSM

A commonly used model of a PMSM is mathematical model in stationary reference frame discretized by simple first-order Euler formula for time step $\Delta t$:

$$i_{s\alpha,t+1} = a i_{s\alpha,t} + b\omega_{me,t}\sin\vartheta_{e,t} + u_{s\alpha,t}\frac{\Delta t}{L_s} + \epsilon_{\alpha,t}, \quad (1)$$

$$i_{s\beta,t+1} = a i_{s\beta,t} - b\omega_{me,t}\cos\vartheta_{e,t} + u_{s\beta,t}\frac{\Delta t}{L_s} + \epsilon_{\beta,t}, \quad (2)$$

$$\omega_{me,t+1} = \omega_{me,t} + \epsilon_{\omega,t}, \quad (3)$$

$$\vartheta_{e,t+1} = \vartheta_{e,t} + \omega_{me,t}\Delta t + \epsilon_{\vartheta,t}. \quad (4)$$

Here, $i_{s\alpha}$, $i_{s\beta}$, $u_{s\alpha}$ and $u_{s\beta}$ represent components of stator current and voltage vector in the stationary reference frame, respectively; $\omega_{me}$ is electrical rotor speed and $\vartheta_e$ is electrical rotor position. Constants $a = (1 - \frac{R_s}{L_s}\Delta t)$ and $b = \frac{\Psi_{pm}}{L_s}\Delta t$ are machine dependent with $R_s$ and $L_s$ being stator resistance and inductance respectively, $\Psi_{pm}$ is the flux linkage excited by permanent magnets on the rotor, and $\Delta t$ is the sampling period. Noise terms $\epsilon_{\alpha,t}, \epsilon_{\beta,t}, \epsilon_{\omega,t}, \epsilon_{\vartheta,t}$, aggregate errors caused by inaccurate discretization, uncertainties in parameters (e.g. due to temperature changes, saturation), unobserved physical effects (such as the unknown load, dead-time effects, non-linear voltage drops on power electronics devices). Equation (3) is simplified, we assume that the speed change within one sampling period is negligible.

Equations (1)–(4) represent non-linear state-space model of PMSM with state vector $x_t = [i_{s\alpha,t}, i_{s\beta,t}, \omega_{me,t}, \vartheta_{e,t}]$. For consistency with the extended Kalman filter assumptions, all of these errors are assumed to influence the state equations as an additive noise with Gaussian distribution. Generally it is assumed that the noise between the state variables is uncorrelated and its variance is constant, $Q = \mathrm{diag}(q_i, q_i, q_\omega, q_\vartheta)$. In sensorless control it is assumed that only two state variables, $i_{\alpha,t}$ and $i_{\beta,t}$ are measured via observations $\bar{i}_{\alpha,t}$ and $\bar{i}_{\beta,t}$:

$$\bar{i}_{s,\alpha} = i_{s,\alpha} + e_{\alpha,t}, \;\; \bar{i}_{s,\beta} = i_{s,\beta} + e_{\beta,t}. \tag{5}$$

Once again, the measurement errors are assumed to be non-correlated Gaussian with variances $var(e_{\alpha,t}) = r_i$, $var(e_{\beta,t}) = r_i$. Equations (1)–(4) are then interpreted as the state equations, while equations (5) are interpreted as the observation equations in the standard EKF implementations. Various techniques of model order reduction has been applied to this model, [8], [7].

In this paper, we propose a simple reduction based on substitution of (5) into (1)–(2). After trivial algebraic manipulation, we obtain

$$\bar{i}_{s\alpha,t+1} = a\bar{i}_{s\alpha,t} + b\omega_{me,t}\sin\vartheta_{e,t} + u_{s\alpha,t}\frac{\Delta t}{L_s} + \xi_{\alpha,t}, \tag{6}$$

$$\bar{i}_{s\beta,t+1} = a\bar{i}_{s\beta,t} - b\omega_{me,t}\cos\vartheta_{e,t} + u_{s\beta,t}\frac{\Delta t}{L_s} + \xi_{\beta,t}. \tag{7}$$

where the error terms are

$$\xi_{\alpha,t} = -ae_{\alpha,t} + e_{\alpha,t+1} + \epsilon_{\alpha,t},$$
$$\xi_{\beta,t} = -ae_{\beta,t} + e_{\beta,t+1} + \epsilon_{\beta,t}.$$

Since all $e_\cdot$and $\epsilon_\cdot$are zero mean Gaussian noises, the $\xi_\cdot$ are also zero-mean Gaussian with variances

$$var(\xi_{\alpha,t}) = var(\xi_{\beta,t}) = [1 + a^2]q_i + r_i. \tag{8}$$

The reduced order model of PMSM is then described by state-equations (3)–(4) and measurement equations (6)–(7). The state variable of the reduced-order model is $x_t = [\omega_{me,t}, \vartheta_{e,t}]$ and the observation variable is $y_t = [\bar{i}_{s\alpha,t}, \bar{i}_{s\beta,t}]$. Stator voltages $u_{s\alpha,t}, u_{s\beta,t}$ are not measured directly but they are reconstructed from measured dc-link voltage and known switching combination of a voltage source inverter supplying a PMSM. Under this interpretation, the classical EKF filter equations:

$$P_t^- = AP_{t-1}^+A^T + Q_t, \tag{9}$$
$$K_t = P_t^-C_t(C_tP_t^-C_t^T + R)^{-1}, \tag{10}$$
$$P_t^+ = (I - K_tC_t)P_t^-, \tag{11}$$
$$\hat{x}_t = A\hat{x}_{t-1} + K_t(y_t - \hat{y}_{t-1}). \tag{12}$$

are now operating on $2\times 2$ matrices $P_t^-$ and $P_t^+$, and matrices

$$A = \begin{bmatrix} 1 & 0 \\ \Delta t & 1 \end{bmatrix}, \quad C_t = \begin{bmatrix} b\sin\hat{\vartheta}_{e,t} & b\hat{\omega}_{me,t}\cos\hat{\vartheta}_{e,t} \\ -b\cos\hat{\vartheta}_{e,t} & b\hat{\omega}_{me,t}\sin\hat{\vartheta}_{e,t} \end{bmatrix},$$

are obtained as derivatives of (3)–(4) and (6)–(7), respectively. We note the following:

- The above interpretation is not a suitable state-space model for control since it is uncontrollable (the state does not depend on $u_{s\alpha,t}$ and $u_{s\beta,t}$). However, it is a valid model for estimation since it is observable.
- This reduced order model was first used in [10].
- The covariances of the reduced-order observation equations (8) are greater than these of the full model.

## III. Fixed-point Implementation of the EKF

Implementation of the EKF equations in fixed-point arithmetics is significantly more demanding than in the floating-point arithmetics. First, it requires to scale the variables to bounded range which may be non-trivial for complex algorithms. Second, the round-off errors are generally greater than those in the floating-point arithmetics and they propagate through the equations to the next step.

Finding suitable ranges for the state variables and the observed variables is straightforward. All these quantities have physical bounds which allows us to establish identities of the kind

$$\omega_{me}^{fix} = \frac{\omega_{me}}{\omega_{me}^{max}} \in < -1, 1 > . \tag{13}$$

Substituting identities (13) for all variables, we obtain $A^{fix}$,$C^{fix}$. However, for $a = 1$, the predicted variance of $\vartheta_{e,t}$ is from (9)

$$P_{\vartheta\vartheta,t}^- = \Delta t^2 P_{\omega\omega,t-1}^+ + 2\Delta t P_{\omega\vartheta,t-1}^+ + P_{\vartheta\vartheta,t-1}^+ + q_\vartheta,$$

where all variances and covariances are positive and thus $P_{\vartheta\vartheta,t}^- > P_{\vartheta\vartheta,t-1}^+$. In the low-speed region the Kalman gain does not decrease $P_{\vartheta\vartheta,t}^-$ and it keeps growing without bounds, see [11] for the associated Cramer-Rao bounds. This can not be implemented in fixed point arithmetics and a bound on $P_{\vartheta\vartheta,t}$ has to be set.

Bierman-Thorton algorithm operated on UD decomposition of the covariance matrices $P_t^+$ and $P_t^-$:

$$P_t = U_tD_tU_t^T. \tag{14}$$

Equations (9)–(12) are then reformulated in terms of updating of variables $U_t^-, D_t^-$ to $U_t^+, D_t^+$. The algorithm that computes (9) is known as the Thorton algorithm, while the algorithm computing (10) and (11) is known as Bierman algorithm, see [5] for their derivation.

Fixed-point implementation of the Bierman-Thorton algorithms has to respect the saturation effect on $P_{\vartheta\vartheta,t}$. Note that

$$P_t = \begin{bmatrix} d_\omega + u^2d_\vartheta & ud_\vartheta \\ ud_\vartheta & d_\vartheta \end{bmatrix}, U_t = \begin{bmatrix} 1 & u \\ 0 & 1 \end{bmatrix}, D_t = \begin{bmatrix} d_\omega & \\ & d_\vartheta \end{bmatrix},$$

where $P_{\vartheta\vartheta,t} = d_\vartheta$. Hence, in the element that needs to be bounded in the UD decomposition is $d_\vartheta$ while the values of the remaining elements of $P_t$ should not be affected. This can be easily achieved by bounding $d_\vartheta$ in the Thorton algorithm. No additional saturations are required in the Bierman algorithm which can be implemented using standard rules of fixed-point arithmetics.

In contrast to the full model studied in [6], the reduced-order model does not allow for as many simplification as the full model since the matrix $C$ is not identity.

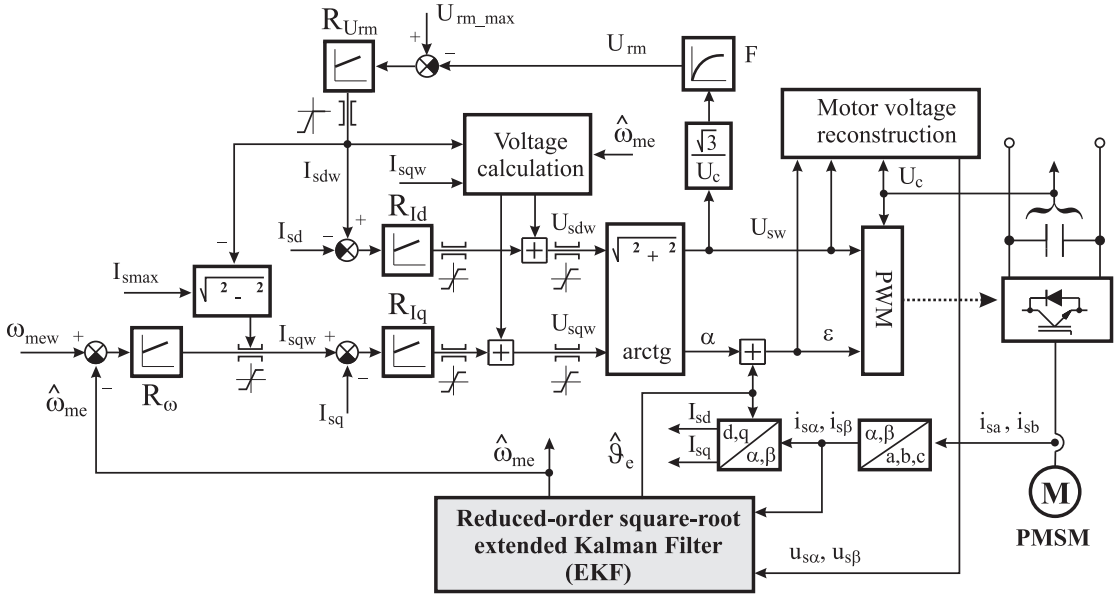


Figure 1. Investigated sensorless control of a PMSM drive with the EKF

## IV. Proposed Sensorless Control of PMSM Drive

Configuration of the investigated sensorless drive control is displayed in Fig. 1. The drive control is based on conventional vector control in Cartesian coordinates in rotating reference frame (d,q) linked to a rotor flux linkage vector. An input to the drive controller is the commanded electrical rotor speed $\omega_{mew}$ which is controlled by PI controller $\mathrm{R}_\omega$. Output of $\mathrm{R}_\omega$ is the demanded torque component $I_{sqw}$ of the stator current vector. The torque ($I_{sqw}$) and flux ($I_{sdw}$) currents are controlled by PI controllers $\mathrm{R_{Isd}}$ and $\mathrm{R_{Isq}}$, respectively. The flux weakening is secured by PI controller $\mathrm{R_{Urm}}$ which controls PWM modulation depth (signal $U_{rm}$) and commands the flux current $I_{sdw}$. The current controllers are supported by block "voltage calculation" (often referred to as "decoupling") which computes the components of the required stator voltage vector in (d,q) frame using a simplified model of the PMSM in steady-state. The components of the stator current vector $(i_{s\alpha}, i_{s\beta})$ and the reconstructed stator voltage vector $u_{s\alpha}, u_{s\beta}$ in stationary reference frame are the inputs to the EKF. The stator voltage vector is reconstructed from measured dc-link voltage and known switching combination of the voltage-source converter. The EKF output is the estimated electrical rotor speed $\hat{\omega}_{me}$ and the electrical rotor position $\hat{\vartheta}_e$. The drive can be operated in two modes: (i) sensored mode (where the drive control uses the rotor speed and position from the rotor position sensor and the EKF is operated in open-loop), and (ii) sensorless mode (where drive control uses the EKF output and hence, EKF is operated in closed-loop). The voltage-source converter employs a third-harmonic injected PWM with carrier frequency of 4kHz. The sampling frequency of the EKF as well as of the drive control has been set to 125$\mu$s.

The proposed sensorless drive control with presented algorithm of the reduced-order square-root EKF (Fig. 1) has been tested on developed prototype of PMSM drive of rated power of 10.7kW. The drive control has been implemented in a fixed-point digital signal processor Texas Instruments TMS320F2812.

Table I
Measured execution time of variants of the EKF on DSP Texas Instruments TMS320F2812 with clock frequency of 150MHz

| time in $\mu$s | full model | reduced model |
|---|---|---|
| Full matrices | 78 | 37 |
| Bierman-Thorton | 77 | 23 |

## V. Simulation Results

Simulation model of the PMSM drive has been designed and implemented in the C language. The "physical" model of a surface-mounted PMSM is represented by state-space model in the stationary reference frame which has been solved using Adams-Bashforth difference formula of 4th order with sampling period of 1$\mu$s. The voltage-source inverter model respects as close as possible dead-time effects (the dead-times have been set to 3$\mu$s which corresponds to those of the laboratory prototype) and non-linear voltage drops on power electronics devices (the power devices are modeled using approximations of their V-A characteristics). The implemented control strategy and the EKF algorithms respect behavior of a real microcontroller-based control system including realistic sampling, known transport delays and finite calculation times. The sampling period of the control and EKF has been, as defined above, set to 125$\mu$s.

Fig. 2 analyzes behavior of the proposed reduced-order square-root EKF algorithm under speed reversal effect. The square-root EKF using reduced-order model was compared with two variants of EKF for the full-order model: (i) the Bierman-Thorton EKF [6], and (ii) the conventional full-covariance matrices EKF [12]. In all tests, the drive was

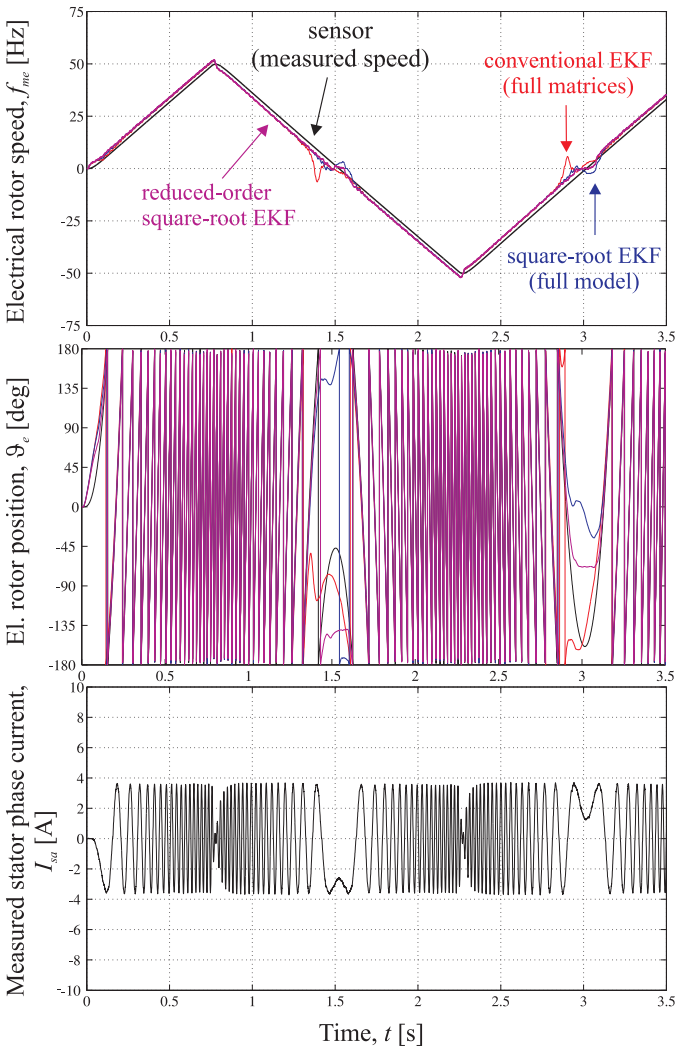


Figure 2. Behavior of the reduced-order square-root EKF algorithm and its comparison with two full-model EKF variants (the Bierman-Thorton EKF and the conventional EKF with full covariance matrices): speed reversal effect, triangular speed profile, commanded el. rotor speed of $f_{mew} = \pm 50$Hz

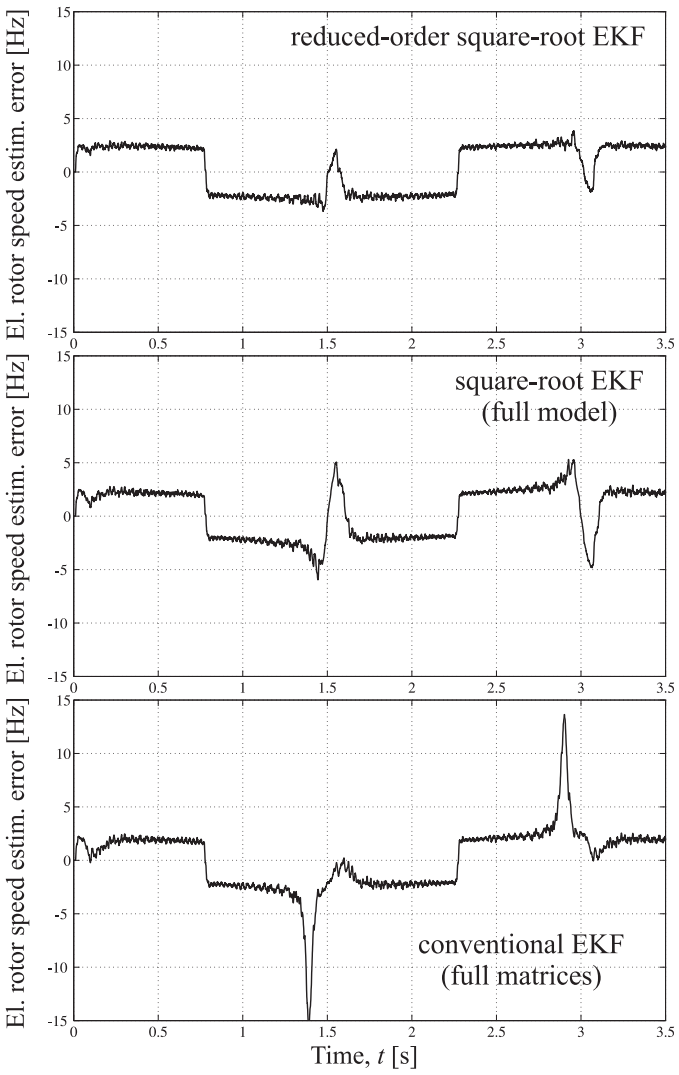


Figure 3. Error of electrical rotor speed estimation for all investigated EKF algorithms: simulation scenario displayed in Fig. 2.

operated in sensored mode, i.e. the control employed rotor speed and position feedback from the rotor position sensor. All EKF algorithms were computed during the simulation test in parallel. Errors of estimation of the electrical rotor speed by particular EKF algorithms are displayed in Fig. 3. From the presented simulation results, it can be concluded that the estimation error of both introduced reduced-order and full-order square-root EKF is almost the same. The filter with reduced-order model achieved a little bit better result in the simulation. The speed estimation error of the new filter is below 5 electrical degrees in the entire speed range including critical low speeds. The presented solution significantly outperforms the conventional EKF with full covariance matrices which had the biggest speed estimation error.

## VI. Experimental Results

The developed prototype of a PMSM drive was in all presented experiments operated in the sensorless control mode. First, we have tested capabilities of the described reduced-order square-root EKF algorithm in the low-speed region. Fig. 4 shows a start of the drive from standstill and the step change of commanded electrical rotor speed from zero to 3Hz. In the next test which is documented in Fig. 5, we have investigated drive behavior under speed reversal effect. The drive was operated under triangular speed profile with the commanded electrical rotor speed of $f_{mew} = \pm 50$ Hz. We have purposely employed quite slow speed ramp to verify the properties of the analyzed EKF algorithm in the critical low-speed region. In order to be able to point out the features of introduced reduced-order square-root EKF, Fig. 6 and Fig. 7 present the behavior of the drive with full-order square-root EKF estimator. The algorithms of square-root EKF for full-order model are in detail described and analyzed in [6]. The reduced-order EKF was to secure a reliable drive operation at higher rotor speeds than the full-order EKF. While the full-order EKF allows robust sensorless drive control from the electrical rotor speed

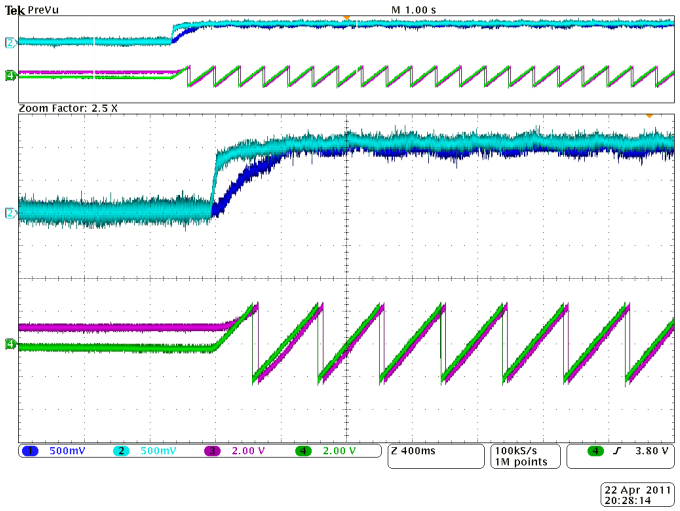


Figure 4. Reduced-order square-root EKF – Step change of electrical rotor speed $f_{mew}$= 0 → 3Hz: initial rotor position is different from the EKF initial condition. ch1: electrical rotor speed (sensor) [0.625 Hz/div], ch2: estimated electrical rotor speed (EKF) [0.625 Hz/div], ch3: electrical rotor position (sensor) [144 deg/div], ch4: estimated electrical rotor position (EKF) [144 deg/div], time scale: 400 ms/div

a) Overlapped waveforms (channels)

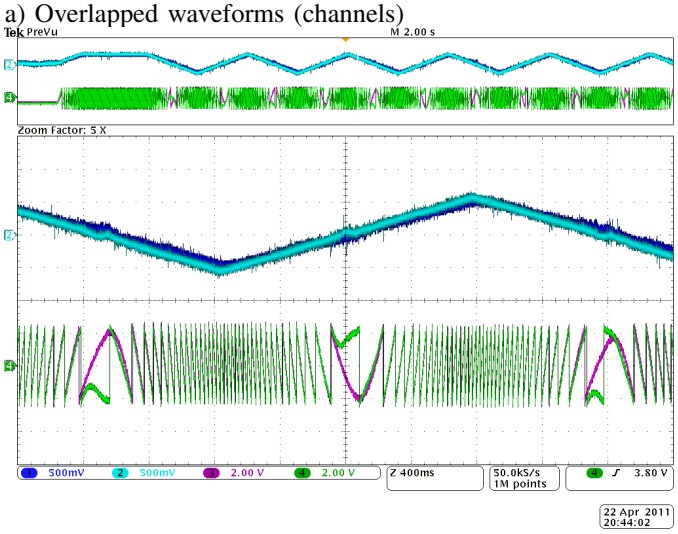


b) The same transient effect with distributed channels

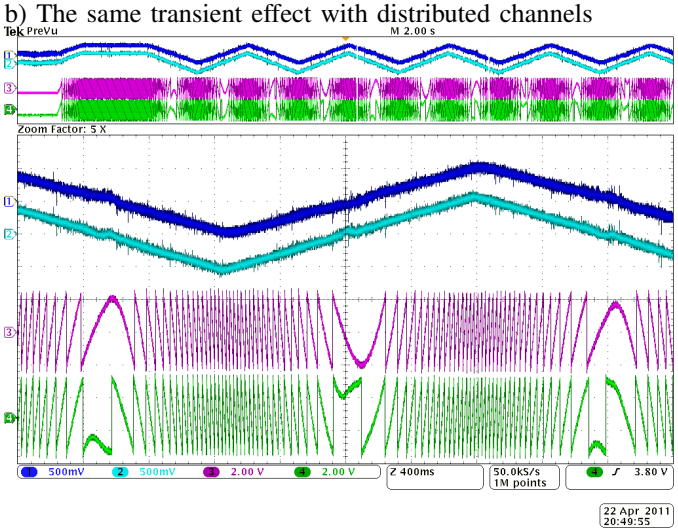


Figure 5. Reduced-order square-root EKF – speed reversal: triangular speed profile, commanded electrical rotor speed $f_{mew} = \pm 50$ Hz. ch1: electrical rotor speed (sensor) [40 Hz/div], ch2: estimated electrical rotor speed (EKF) [40 Hz/div], ch3: electrical rotor position (sensor) [144 deg/div], ch4: estimated electrical rotor position (EKF) [144 deg/div], time scale: 400 ms/div

over 1.8Hz (27 rpm), the reduced-order EKF secures the robust drive operation from electrical rotor speed over 3Hz (45 rpm). From the analysis of the drive speed reversal can be concluded that EKF with full model achieved almost the same transition through critical low speed region. The proposed reduced-order square-root EKF achieved very good steady-state precision and cultivated transitions through the low-speed region. Therefore, reduced-order EKF represents fully competitive solution to the EKF with full-order model in terms of precision of the state estimation. However, computational time of the reduced-order algorithm is more than 3 times shorter than that of the original full-order estimators. Execution times of all variants of the EKF measured with DSP clock frequency of 150MHz are displayed in Table I.

## VII. Conclusion

Fixed-point implementation of the square-root EKF based on reduced-order model was presented and its performance tested by simulations and experiments carried out on developed laboratory prototype of PMSM drive of 10.7kW. Specifically, we have tested and compared Bierman-Thorton algorithm of EKF for the reduced-order model and the conventional full model. We have found that the reduced-order model is fully comparable with the full order model in terms of both static and dynamic properties. The reduced-order model has fewer elements in the covariance matrix, and is far less sensitive to their choice which simplifies the task of their tuning. On the other hand, more richer covariance structure of the full model allows finer tuning of its performance, which has been demonstrated by achieving reliable performance at lower speed that the reduced model. The most attractive property of the reduced order model is more than 3 times shorter computation time. Hence, it can be computed without significant difficulties on a common fixed-point DSPs which are currently used in industry. This makes the proposed reduced-order square-root EKF an eligible solution for diagnostic systems as well as sensorless control of ac motor drives in a wide range of industrial applications.

## Acknowledgement

This work was supported by the European Regional Development Fund and Ministry of Education, Youth and Sports of the Czech Republic under project No. CZ.1.05/2.1.00/03.0094: Regional Innovation Centre for Electrical Engineering (RICE) and by the Czech Science Foundation under project No. P102/11/0437.

## References

[1] T. Orlowska-Kowalska and M. Dybkowski, "Stator-current-based mras estimator for a wide range speed-sensorless induction-motor drive,"

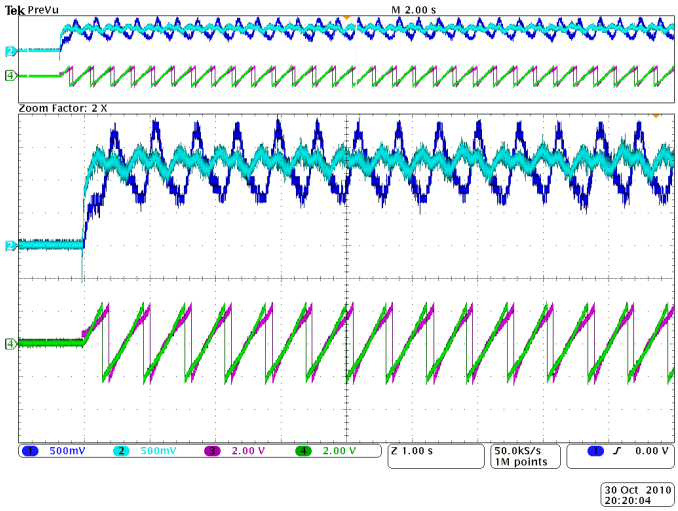


Figure 6. Square-root EKF with full order model – Step change of electrical rotor speed $f_{mew}$= 0 $\rightarrow$ 1.8Hz: initial rotor position is different from the EKF initial condition. ch1: electrical rotor speed (sensor) [0.625 Hz/div], ch2: estimated electrical rotor speed (EKF) [0.625 Hz/div], ch3: electrical rotor position (sensor) [144 deg/div], ch4: estimated electrical rotor position (EKF) [144 deg/div], time scale: 1 s/div1.8Hz

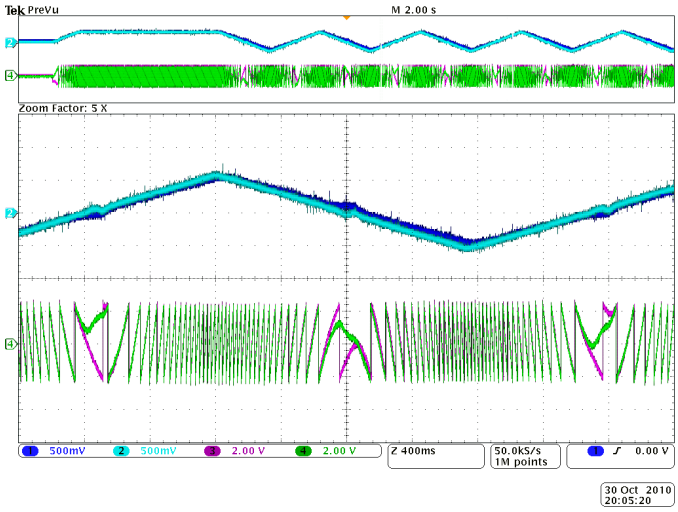


Figure 7. Square-root EKF with full order model – speed reversal: triangular speed profile, commanded electrical rotor speed $f_{mew} = \pm 50$ Hz. ch1: electrical rotor speed (sensor) [40 Hz/div], ch2: estimated electrical rotor speed (EKF) [40 Hz/div], ch3: electrical rotor position (sensor) [144 deg/div], ch4: estimated electrical rotor position (EKF) [144 deg/div], time scale: 400 ms/div

*Industrial Electronics, IEEE Transactions on*, vol. 57, no. 4, pp. 1296–1308, 2010.

[2] R. Dhaouadi, N. Mohan, and L. Norum, "Design and implementation of an extended Kalman filter for the state estimation of a permanent magnet synchronous motor," *Power Electronics, IEEE Transactions on*, vol. 6, no. 3, pp. 491–497, 1991.

[3] S. Bolognani, R. Oboe, and M. Zigliotto, "Sensorless full-digital PMSM drive with EKF estimation of speed and rotor position.," *IEEE Trans. on Industrial Electronics*, vol. 46, pp. 184 – 191, 1999.

[4] L. Idkhajine, E. Monmasson, and A. Maalouf, "Extended kalman filter for ac drive sensorless speed controller - fpga-based solution or dsp-based solution," in *Industrial Electronics (ISIE), 2010 IEEE International Symposium on*, pp. 2759–2764, 2010.

[5] M. Grewal and A. Andrews, *Kalman filtering: theory and practice using MATLAB*. Wiley-IEEE Press, 2008.

[6] V. Šmídl and Z. Peroutka, "Advantages of square-root extended kalman filter for sensorless control of ac drives," *IEEE Transactions on Industrial Electronics*, 2011. submitted for publication.

[7] J. Kim and S. Sul, "High performance PMSM drives without rotational position sensors using reduced order observer," in *Industry Applications Conference, 1995. Thirtieth IAS Annual Meeting, IAS'95., Conference Record of the 1995 IEEE*, vol. 1, pp. 75–82, IEEE, 1995.

[8] M. Huang, A. Moses, F. Anayi, and X. Yao, "Reduced-Order Linear Kalman Filter (RLKF) Theory in Application of Sensorless Control for Permanent Magnet Synchronous Motor (PMSM)," in *Industrial Electronics and Applications, 2006 1ST IEEE Conference on*, pp. 1–6, IEEE, 2006.

[9] D.-H. Yim, B.-G. Park, and D.-S. Hyun, "Sensorless control strategy of ipmsm based on a parallel reduced-order ekf," in *IECON 2010 - 36th Annual Conference on IEEE Industrial Electronics Society*, pp. 2258–2263, nov. 2010.

[10] B. Nahid-Mobarakeh, F. Meibody-Tabar, and P. Sargos, "State and disturbance observers in mechanical sensorless control of PMSM," in *Industrial Technology, 2004. IEEE ICIT'04. 2004 IEEE International Conference on*, vol. 1, pp. 181–186, IEEE, 2004.

[11] Z. Peroutka, V. Šmídl, and D. Vošmik, "Challenges and limits of extended kalman filter based sensorless control of permanent magnet synchronous machine drives," in *Proc. of the 13th European Conference on Power Electronics and Applications*, (Barcelona, Spain), 2009.

[12] Z. Peroutka, "Development of sensorless PMSM drives: Application of extended kalman filter," in *Proc. of IEEE Int. Symposium on Industrial Electronics*, (Dubrovnik, Croatia), pp. 1647 – 1652, 2005.